Journal of Quantitative Spectroscopy & Radiative Transfer 183 (2016) 78–84

Contents lists available at ScienceDirect

Journal of Quantitative Spectroscopy & Radiative Transfer

journal homepage: www.elsevier.com/locate/jqsrt

Notes

# Expansion of tabulated scattering matrices in generalized spherical functions

Michael I. Mishchenko [a,*], Igor V. Geogdzhayev [b], Ping Yang [c]

[a] NASA Goddard Institute for Space Studies, 2880 Broadway, New York, NY 10025, USA
[b] Columbia University, Department of Applied Physics and Applied Mathematics/NASA GISS, 2880 Broadway, New York, NY 10025, USA
[c] Department of Atmospheric Sciences, Texas A&M University, College Station, TX 77843, USA

ARTICLE INFO

*Article history:*
Received 28 April 2016
Received in revised form
12 May 2016
Accepted 13 May 2016
Available online 21 May 2016

*Keywords:*
Electromagnetic scattering
Polarization
Scattering matrix
Generalized spherical functions
Radiative transfer
Stokes parameters

ABSTRACT

An efficient way to solve the vector radiative transfer equation for plane-parallel turbid media is to Fourier-decompose it in azimuth. This methodology is typically based on the analytical computation of the Fourier components of the phase matrix and is predicated on the knowledge of the coefficients appearing in the expansion of the normalized scattering matrix in generalized spherical functions. Quite often the expansion coefficients have to be determined from tabulated values of the scattering matrix obtained from measurements or calculated by solving the Maxwell equations. In such cases one needs an efficient and accurate computer procedure converting a tabulated scattering matrix into the corresponding set of expansion coefficients. This short communication summarizes the theoretical basis of this procedure and serves as the user guide to a simple public-domain FORTRAN program.

Published by Elsevier Ltd.

## 1. Introduction

An efficient way of solving the vector radiative transfer equation (VRTE) for plane-parallel turbid media composed of statistically isotropic and mirror-symmetric random particles [1,2] is to Fourier-decompose the VRTE in azimuth and find each Fourier component separately (see, e.g., [3–20] and references therein). The central element of this methodology is the analytical procedure for the computation of the Fourier components of the phase matrix using the addition theorem for generalized spherical functions (GSFs). This procedure dates back to the seminal papers by Kuščer and Ribarič [21], Domke [22], Siewert [23,24], and Hovenier and van der Mee [25]. The most convenient version of this procedure based on real-valued Stokes parameters was developed by de Haan et al. [5] and summarized by Hovenier et al. [26]. Their approach is based on the underlying expansion of the corresponding normalized scattering matrix [1,2] in appropriate GSFs and is thus predicated on the knowledge of the corresponding expansion coefficients for the particle ensemble in question.

There are several numerical techniques for the explicit computation of the expansion coefficients for specific particle types based on such direct solvers of the macroscopic Maxwell equations as the Lorenz–Mie theory and the (superposition) *T*-matrix method. In particular, direct computations of the expansion coefficients bypassing the prior computation of the scattering matrix can be performed for

- monodisperse or polydisperse homogeneous and radially inhomogeneous spherical particles [27–31];
- monodisperse or polydisperse, randomly oriented homogeneous spheroids, circular cylinders, and regular 2D Chebyshev particles [30,32];
- monodisperse bispheres [33];
- clusters of separated, externally touching, and/or nested spheres [34–36].

* Corresponding author. Fax: +1 212 678 5222.
*E-mail address:* michael.i.mishchenko@nasa.gov (M.I. Mishchenko).

http://dx.doi.org/10.1016/j.jqsrt.2016.05.015
0022-4073/Published by Elsevier Ltd.

Several FORTRAN computer programs based on these techniques are publicly available on-line [37]. Other nonspherical shapes such as polyhedral particles, regular 3D Chebyshev particles, and 2D and 3D Gaussian random spheres can be handled using the *T*-matrix code described in [38] and also publicly available on-line [39]. Of course, these public-domain computer programs may be inapplicable to certain particle morphologies and/or size-parameter ranges. In many such cases one may be able to use the core-mantle and invariant-imbedding *T*-matrix programs described in [40–43].

Quite often however the expansion coefficients cannot be computed directly and must be determined from tabulated values of the scattering matrix elements. This happens when the scattering matrix is measured experimentally [44–48] or is computed using alternative numerical techniques such as, for example, the ray tracing (or geometrical optics) approximation [49–57], the discrete-dipole approximation [58–61], the finite-difference time-domain method [62–64], and the pseudo-spectral time domain method [65,66] (see also Refs. [67–74]). In such cases it is essential to have an efficient, accurate, and user-friendly computer procedure converting a tabulated scattering matrix into the corresponding set of expansion coefficients. The main objective of this short communication is to summarize the theoretical basis of this procedure and serve as the user guide to a simple public-domain FORTRAN program.

To make the discussion more compact, we will use throughout the terminology and notation adopted in the monographs [1,2,30]. Note that [1,30] are available on-line as PDF files at ⟨http://www.giss.nasa.gov/staff/mmishchenko/books.html⟩ as well as at https://www.researchgate.net/profile/Michael_Mishchenko.

## 2. Expansion of the scattering matrix in generalized spherical functions

We assume that the random particles forming a sparse turbid layer are statistically isotropic and mirror symmetric [1,2,26,30]. This means that all orientations of a particle are equally probable. Furthermore, each particle has a plane of symmetry and/or is accompanied by its mirror counterpart.

This assumption allows us to fully characterize the single-scattering properties of the particulate medium by the ensemble-averaged single-scattering albedo $\varpi$ and so-called normalized $4\times 4$ Stokes scattering matrix $\tilde{\mathbf{F}}(\Theta)$ with real-valued components. The latter has the well-known block-diagonal structure:

$$\tilde{\mathbf{F}}(\Theta)=\begin{bmatrix} a_1(\Theta) & b_1(\Theta) & 0 & 0 \\ b_1(\Theta) & a_2(\Theta) & 0 & 0 \\ 0 & 0 & a_3(\Theta) & b_2(\Theta) \\ 0 & 0 & -b_2(\Theta) & a_4(\Theta) \end{bmatrix}, \tag{1}$$

where $\Theta \in [0,\ \pi]$ is the angle between the incidence and scattering directions (i.e., the scattering angle). The (1,1) element (called the phase function) is non-negative and satisfies the normalization condition

$$\frac{1}{2}\int_0^\pi \mathrm{d}\Theta\ \sin\Theta\ a_1(\Theta)=1. \tag{2}$$

The elements of the normalized scattering matrix (1) can be expanded in GSFs $P^s_{mn}(\cos\Theta)$ [1,2,26,30]:

$$a_1(\Theta)=\sum_{s=0}^{s_{\max}}\alpha_1^s P^s_{00}(\cos\Theta), \tag{3}$$

$$a_2(\Theta)+a_3(\Theta)=\sum_{s=0}^{s_{\max}}(\alpha_2^s+\alpha_3^s)P^s_{22}(\cos\Theta), \tag{4}$$

$$a_2(\Theta)-a_3(\Theta)=\sum_{s=0}^{s_{\max}}(\alpha_2^s-\alpha_3^s)P^s_{2,-2}(\cos\Theta), \tag{5}$$

$$a_4(\Theta)=\sum_{s=0}^{s_{\max}}\alpha_4^s P^s_{00}(\cos\Theta), \tag{6}$$

$$b_1(\Theta)=\sum_{s=0}^{s_{\max}}\beta_1^s P^s_{02}(\cos\Theta), \tag{7}$$

$$b_2(\Theta)=\sum_{s=0}^{s_{\max}}\beta_2^s P^s_{02}(\cos\Theta), \tag{8}$$

where the upper summation limit $s_{\max}$ depends on the requisite numerical accuracy. Note that these expansions can also be written in terms of real-valued so-called Wigner *d*-functions given by

$$d^s_{mn}(\Theta)=\mathrm{i}^{n-m}P^s_{mn}(\cos\Theta) \tag{9}$$

(see [75] and Appendix F in [1]).

If the normalized scattering matrix is known beforehand, the expansion coefficients can be calculated by evaluating the following integrals:

$$\alpha_1^s=(s+\tfrac{1}{2})\int_0^\pi \mathrm{d}\Theta\ \sin\Theta\ a_1(\Theta)\,d^s_{00}(\Theta), \tag{10}$$

$$\alpha_2^s+\alpha_3^s=(s+\tfrac{1}{2})\int_0^\pi \mathrm{d}\Theta\ \sin\Theta\ [a_2(\Theta)+a_3(\Theta)]\ d^s_{22}(\Theta), \tag{11}$$

$$\alpha_2^s-\alpha_3^s=(s+\tfrac{1}{2})\int_0^\pi \mathrm{d}\Theta\ \sin\Theta\ [a_2(\Theta)-a_3(\Theta)]\ d^s_{2,-2}(\Theta), \tag{12}$$

$$\alpha_4^s=(s+\tfrac{1}{2})\int_0^\pi \mathrm{d}\Theta\ \sin\Theta\ a_4(\Theta)\,d^s_{00}(\Theta), \tag{13}$$

$$\beta_1^s=-(s+\tfrac{1}{2})\int_0^\pi \mathrm{d}\Theta\ \sin\Theta\ b_1(\Theta)\,d^s_{02}(\Theta), \tag{14}$$

$$\beta_2^s=-(s+\tfrac{1}{2})\int_0^\pi \mathrm{d}\Theta\ \sin\Theta\ b_2(\Theta)\,d^s_{02}(\Theta). \tag{15}$$

These formulas follow from Eqs. (3)–(9) and the orthogonality property of the Wigner *d*-functions [1,75].

## 3. Numerical integration

As we have already mentioned, in some cases the expansion coefficients can be calculated directly without computing explicitly the elements of the scattering matrix. Alternatively, one needs to evaluate the integrals (10)–(15) numerically by using a quadrature formula. By virtue of being exact for all polynomials of degree $2N_{\mathrm{G}}-1$ or lower, where $N_{\mathrm{G}}$ is the number of quadrature nodes, the classical Gaussian

quadrature formula represents by far the best practical choice [76]. We thus have

$$\alpha_1^s \approx (s+\tfrac{1}{2})\sum_{j=1}^{N_G} w_j a_1(\arccos\mu_j) d_{00}^s(\arccos\mu_j), \tag{16}$$

$$\alpha_2^s+\alpha_3^s \approx (s+\tfrac{1}{2})\sum_{j=1}^{N_G} w_j \left[a_2(\arccos\mu_j)+a_3(\arccos\mu_j)\right] d_{22}^s(\arccos\mu_j), \tag{17}$$

$$\alpha_2^s-\alpha_3^s \approx (s+\tfrac{1}{2})\sum_{j=1}^{N_G} w_j \left[a_2(\arccos\mu_j)-a_3(\arccos\mu_j)\right] d_{2,-2}^s(\arccos\mu_j), \tag{18}$$

$$\alpha_4^s \approx (s+\tfrac{1}{2})\sum_{j=1}^{N_G} w_j a_4(\arccos\mu_j) d_{00}^s(\arccos\mu_j), \tag{19}$$

$$\beta_1^s \approx -(s+\tfrac{1}{2})\sum_{j=1}^{N_G} w_j b_1(\arccos\mu_j) d_{02}^s(\arccos\mu_j), \tag{20}$$

$$\beta_2^s \approx -(s+\tfrac{1}{2})\sum_{j=1}^{N_G} w_j b_2(\arccos\mu_j) d_{02}^s(\arccos\mu_j), \tag{21}$$

where $\mu_j$ and $w_j$ are the Gaussian quadrature nodes and weights on the interval $[-1,\ 1]$ and $N_G = s_{max}$.

To compute the Wigner $d$-functions entering Eqs. (16)–(21), we use the following recurrence relation [75]:

$$\begin{aligned} d_{mn}^{s+1}(\theta) = {} & \frac{1}{s\sqrt{(s+1)^2-m^2}\sqrt{(s+1)^2-n^2}} \\ & \times\{(2s+1)[s(s+1)\cos\theta - mn] d_{mn}^s(\theta) \\ & -(s+1)\sqrt{s^2-m^2}\sqrt{s^2-n^2}\, d_{mn}^{s-1}(\theta)\}, \end{aligned} \tag{22}$$

where $s \geq s_{min}$ and

$$s_{min} = \max(|m|, |n|). \tag{23}$$

Note that in general, $d_{mn}^s(\theta) \equiv 0$ for $s < s_{min}$. The initial values for the recurrence relation (22) are given by

$$d_{mn}^{s_{min}-1}(\theta) = 0, \tag{24}$$

$$\begin{aligned} d_{mn}^{s_{min}}(\theta) = {} & \xi_{mn} 2^{-s_{min}} \left[\frac{(2s_{min})!}{(|m-n|)!(|m+n|)!}\right]^{1/2} \\ & \times(1-\cos\theta)^{|m-n|/2}(1+\cos\theta)^{|m+n|/2}, \end{aligned} \tag{25}$$

where

$$\xi_{mn} = \begin{cases} 1 & \text{for } n \geq m, \\ (-1)^{m-n} & \text{for } n < m. \end{cases} \tag{26}$$

It is imperative to recognize that the normalization condition (2) requires the expansion coefficient $\alpha_1^0$ to be identically equal to unity:

$$\alpha_1^0 \equiv 1. \tag{27}$$

Even small deviations from this identity in radiative-transfer computations for optically thick particulate layers can lead to large numerical errors. Therefore, the final step in the computation of the expansion coefficients according to Eqs. (16)–(21) is the calculation of the normalization coefficient

$$C = \frac{1}{\alpha_1^0} \tag{28}$$

and the subsequent multiplication of all the expansion coefficients $\alpha_1^s$, $\alpha_2^s$, $\alpha_3^s$, $\alpha_4^s$, $\beta_1^s$, and $\beta_2^s$ by this coefficient.

The deviation of $C$ from unity should be considered an important indicator of numerical accuracy of the resulting expansion coefficients and, in fact, of the accuracy of the input scattering matrix. Typically achieving small $|C-1|$ values requires a careful treatment of the diffraction peak in the diagonal elements of the scattering matrix, e.g., tabulating it with very high angular resolution.

## 4. FORTRAN procedure

The public-domain FORTRAN procedure for the calculation of the expansion coefficients is partitioned into two files: `sphere_expan.f` and `params.h`. The first one combines the main program and all relevant subroutines, while the second one contains user-defined parameters. These files are available at [77]. Both files must reside in the same directory during the execution of the program.

A file `input_file_name` tabulating the six nonzero elements of the scattering matrix (1) for a set of scattering angles serves as the input. The data should be arranged in seven columns as follows:

$$\begin{array}{cccccccc} \Theta_1 & a_1(\Theta_1) & a_2(\Theta_1) & a_3(\Theta_1) & a_4(\Theta_1) & b_1(\Theta_1) & b_2(\Theta_1) \\ \Theta_2 & a_1(\Theta_2) & a_2(\Theta_2) & a_3(\Theta_2) & a_4(\Theta_2) & b_1(\Theta_2) & b_2(\Theta_2) \\ \cdots & & & & & & \\ \Theta_{N_\Theta} & a_1(\Theta_{N_\Theta}) & a_2(\Theta_{N_\Theta}) & a_3(\Theta_{N_\Theta}) & a_4(\Theta_{N_\Theta}) & b_1(\Theta_{N_\Theta}) & b_2(\Theta_{N_\Theta}) \end{array} \tag{29}$$

where $N_\Theta$ is the total number of (increasing) input scattering angles. The typical execution command reads

```
./a.out input_file_name
```  (30)

The result of the execution is a set of two files `input_file_name.expan_coeff` and `input_file_name.expan_matr` tabulating the expansion coefficients and the scattering matrix elements re-expanded according to Eqs. (3)–(8). The latter can be compared with the original input to assess the resulting numerical accuracy. The format of the file `input_file_name.expan_matr` is given by Eq. (29), while that of the file `input_file_name.expan_coeff` is as follows:

$$\begin{array}{cccccccc} s_{max} & C & & & & & & \\ 0 & \alpha_1^0 & \alpha_2^0 & \alpha_3^0 & \alpha_4^0 & \beta_1^0 & \beta_2^0 \\ 1 & \alpha_1^1 & \alpha_2^1 & \alpha_3^1 & \alpha_4^1 & \beta_1^1 & \beta_2^1 \\ \cdots & & & & & & \\ s_{max} & \alpha_1^{s_{max}} & \alpha_2^{s_{max}} & \alpha_3^{s_{max}} & \alpha_4^{s_{max}} & \beta_1^{s_{max}} & \beta_2^{s_{max}} \end{array} \tag{31}$$

In order to evaluate the sums (16)–(21), the input scattering matrix should ideally be precomputed at the Gaussian nodes (cf. [28,30]). Otherwise it has to be interpolated to the Gaussian nodes numerically. While polynomial or spline interpolation can be applied to scattering matrices with a smooth angular dependence, it can be problematic in the case of phase functions with a strong forward peak and sharp angular features such as halos exhibited by pristine hexagonal ice crystals. The residual noise in the measured scattering matrix elements can also cause problems. We have therefore decided to use simple

linear interpolation (extrapolation) irrespective of the source of tabulated values of the scattering matrix.

Depending on the nature of the input, the algorithm can operate in either of two modes controlled by the parameter NSPHER. In the first mode a positive integer value of NSPHER prescribes the number $s_{max}$ of the expansion coefficients to be calculated (and thus the number of Gaussian nodes $N_G = s_{max}$ to be used). The second mode is entered if NSPHER is set to a negative value. In that case the number of the expansion coefficients $N_G$ is originally set to MIN_NSPHER and is then increased in steps of DELTA_NG to reduce the discrepancy between the original and the re-expanded scattering matrices to below a user-specified threshold DESIRED_ERR. The user can choose one of three error metrics for the estimation of the numerical discrepancy by specifying the appropriate value of the parameter ERRTYP:

- the maximum absolute difference between the original and expanded phase functions (ERRTYP=MAXABS);
- the maximum absolute relative difference between the original and expanded phase functions (in percent; ERRTYP= MAXPERCENT); or
- the mean square root error of the expanded phase function (ERRTYP=MSRE).

Additionally, the range of scattering angles (in degrees) at which the discrepancy is estimated can be specified by defining the parameters ang_min and ang_max.

Each error metrics can be calculated on the original grid of scattering angles at which the input scattering matrix is specified or on the alternative set of scattering angles calculated by retaining the smallest and the largest original scattering angles and replacing the intermediate angles by the middle points of the intervals formed by pairs of adjacent angles in the original grid. The values of the phase function for the new angles are found by linear interpolation and the discrepancy between the original and the expanded phase functions is calculated for the new set of angles. The purpose of this test is to check whether the requisite accuracy has been achieved for scattering angles other than the original ones. The first mode is entered by specifying any integer value of USE_ALT_ANG other than 1.

## 5. Illustrative example

As an example, we describe the application of the program sphere_expan.f to the scattering matrix of an ice cloud computed using the technique described in [51]. The computation is based on the Moderate Resolution Imaging Spectroradiometer (MODIS) Collection 5 (C5) ice crystal habit model [78] which includes 100% droxtals for $0 < D_{max} < 60$ μm; 15% bullet rosettes, 60% solid columns, and 35% plates for 60 μm $< D_{max} <$ 1000 μm; 45% hollow columns, 45% solid columns, and 10% aggregates for 1000 μm $< D_{max} <$ 2500 μm; and 97% bullet rosettes and 3% aggregates for 2500 μm $< D_{max}$, where $D_{max}$ is the particle's maximum dimension (Fig. 1). In this ice crystal model the particle facets are assumed to be smooth, thereby leading to significant 22° and 46° halos and other pronounced angular features.

It has been suggested that halos are not often observed and the phase function of ice clouds may be rather featureless in many cases [79]. To accommodate this scenario, the newly developed MODIS Collection 6 (C6) ice model assumes ice crystals to be roughened aggregates characterized by a gamma size distribution, which produces featureless phase functions without pronounced halo peaks [80]. Importantly, the MODIS C6 phase function is able to provide spectral consistency between the ice cloud property retrievals based on solar band-based techniques and infrared based methods [80].

Since we want to demonstrate the applicability of the program sphere_expan.f to scattering matrices with sharp angular features, we use the MODIS C5 scattering matrix computed for MODIS channel 1 covering the spectral range 620–670 nm. The solid curves in Fig. 2 show the original MODIS C5 channel-1 scattering matrix corresponding to an effective particle size of $D_{eff}$=60 μm. We first computed the expansion coefficients using the algorithm described above and then used the resulting expansion coefficients to re-calculate the scattering matrix and compare it with the original one. Specifically, the scattering matrix elements were expanded in GSFs using $s_{max} = N_G = 50$ and 5000 coefficients. The re-expanded matrix corresponding to $N_G$=50 is depicted by the dashed curves and reveals a rather poor fit. In particular, this number of the expansion coefficients is grossly insufficient to describe the sharp forward-scattering phase-function peak. Increasing the number of the expansion coefficients to 5000 (the results not shown) yields an essentially perfect fit for the entire range of scattering angles. The resulting normalization coefficient $C$=1.00022 is very close to unity and hence is also indicative of excellent numerical fidelity.

To investigate the rate of numerical convergence in more detail, we calculated the re-expanded phase functions for increasing numbers of the expansion coefficients and computed the mean square root errors between the original and re-expanded phase functions for the entire scattering-angle range. The results are presented in Fig. 3 and demonstrate that increasing the number of the expansion coefficients does

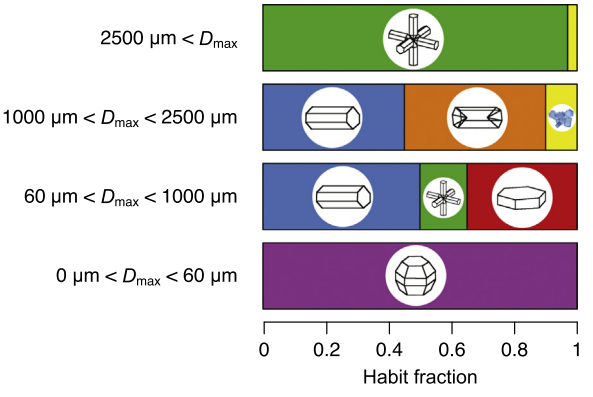


**Fig. 1.** MODIS C5 ice crystal habit model.

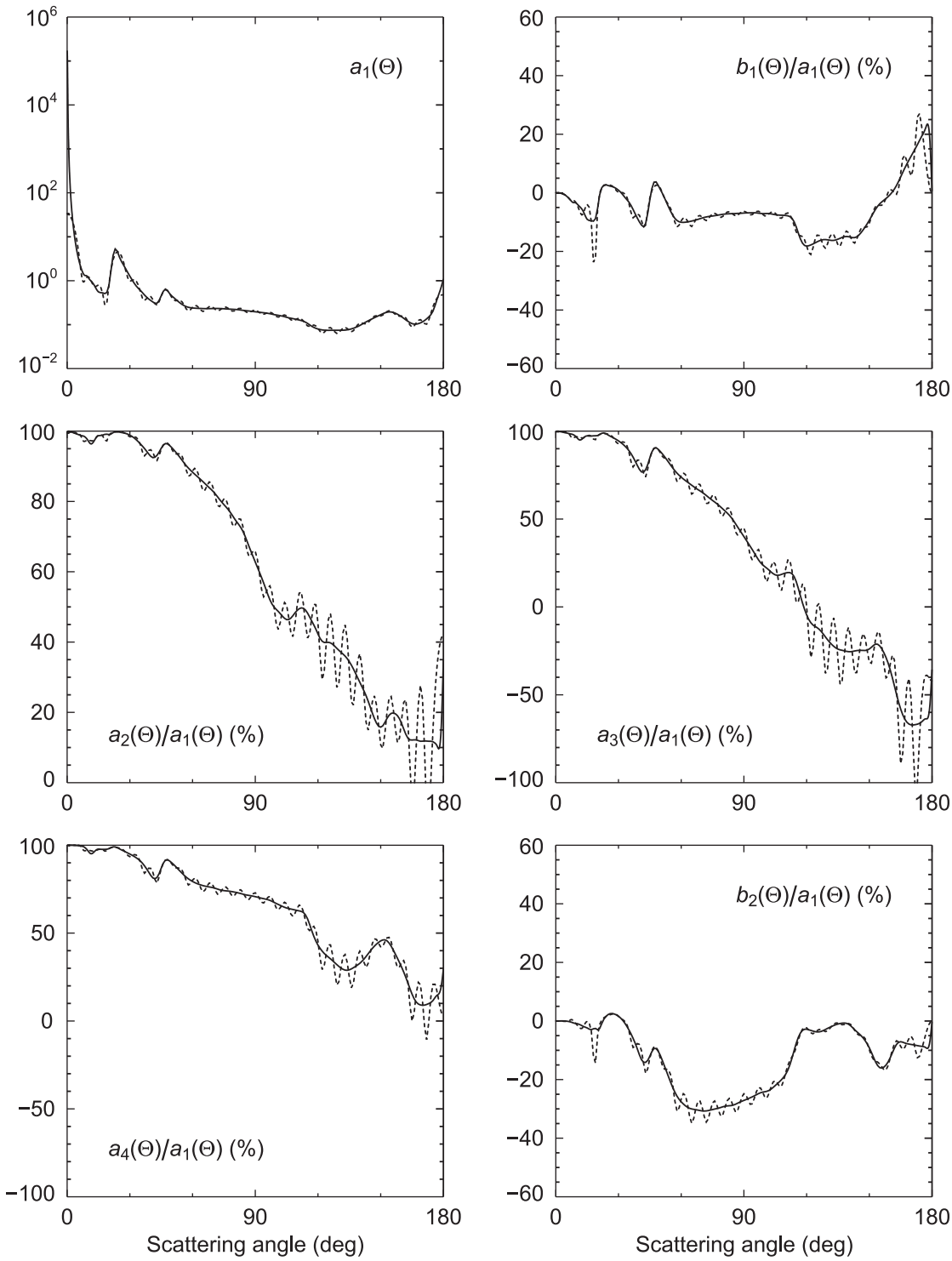


**Fig. 2.** Comparison of the original MODIS channel-1 ice-crystal scattering matrix (solid curves) with the re-expanded one for $s_{max}=50$ (dashed curves).

tend to reduce the error. The reduction is not uniform since shifts of the Gaussian quadrature nodes relative to the angular features of the phase function can occasionally increase the errors as $N_G$ increases. In general, Fig. 3 shows that the initial sharp reduction of the error, which is largely due to improved modeling of the forward-scattering peak, is followed by a much slower overall decrease.

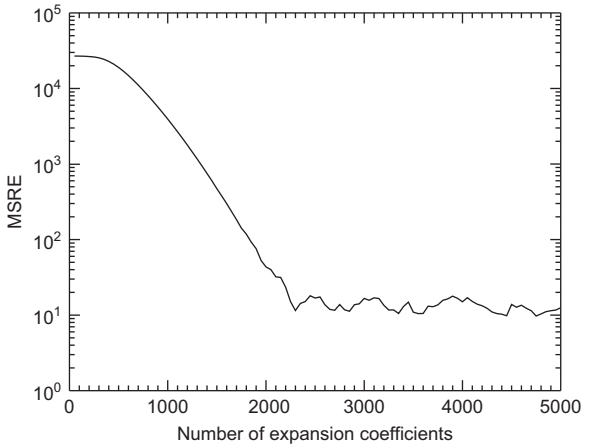


**Fig. 3.** The dependence of the mean square root error on the number of the expansion coefficients.

## Acknowledgments

We thank two anonymous reviewers for constructive suggestions. M.I.M. and I.V.G. acknowledge support from the NASA ACE Project managed by Hal Maring, Paula Bontempi, and Arlindo da Silva.

## References

[1] Mishchenko MI, Travis LD, Lacis AA. Multiple scattering of light by particles: radiative transfer and coherent backscattering. Cambridge, UK: Cambridge University Press; 2006.
[2] Mishchenko MI. Electromagnetic scattering by particles and particle groups: an introduction. Cambridge, UK: Cambridge University Press; 2014.
[3] Hansen JE, Travis LD. Light scattering in planetary atmospheres. Space Sci Rev 1974;16:527–610.
[4] Garcia RDM, Siewert CE. A generalized spherical harmonics solution for radiative transfer models that include polarization effects. J Quant Spectrosc Radiat Trans 1986;36:401–23.
[5] de Haan JF, Bosma PB, Hovenier JW. The adding method for multiple scattering calculations of polarized light. Astron Astrophys 1987;183:371–91.
[6] Mishchenko MI. The fast invariant imbedding method for polarized light: computational aspects and numerical results for Rayleigh scattering. J Quant Spectrosc Radiat Transf 1990;43:163–71.
[7] Evans KF, Stephens GL. A new polarized atmospheric radiative transfer model. J Quant Spectrosc Radiat Trans 1991;46:413–23.
[8] Mishchenko MI, Travis LD. Satellite retrieval of aerosol properties over the ocean using polarization as well as intensity of reflected sunlight. J Geophys Res 1997;102:16989–7013.
[9] Schulz FM, Stamnes K, Weng F. VDISORT: an improved and generalized discrete ordinate radiative transfer model for polarized (vector) radiative transfer computations. J Quant Spectrosc Radiat Transf 1999;61:105–22.
[10] Siewert CE. A discrete-ordinates solution for radiative-transfer models that include polarization effects. J Quant Spectrosc Radiat Transf 2000;64:227–54.
[11] Schulz FM, Stamnes K. Angular distribution of the Stokes vector in a plane-parallel, vertically inhomogeneous medium in the vector discrete ordinate radiative transfer (VDISORT) model. J Quant Spectrosc Radiat Transf 2000;65:609–20.
[12] Hasekamp OP, Landgraf J. A linearized vector radiative transfer model for atmospheric trace gas retrieval. J Quant Spectrosc Radiat Transf 2002;75:221–38.
[13] Spurr RJD. VLIDORT: a linearized pseudo-spherical vector discrete ordinate radiative transfer code for forward model and retrieval studies in multilayer multiple scattering media. J Quant Spectrosc Radiat Transf 2006;102:316–42.
[14] Rozanov VV, Kokhanovsky AA. The solution of the vector radiative transfer equation using the discrete ordinates technique: selected applications. Atmos Res 2006;79:241–65.
[15] Spurr R. LIDORT and VLIDORT: linearized pseudo-spherical scalar and vector discrete ordinate radiative transfer models for use in remote sensing retrieval problems. Light Scatter Rev 2008;3:229–75.
[16] Ota Y, Higurashi A, Nakajima T, Yokota T. Matrix formulations of radiative transfer including the polarization effect in a coupled atmosphere–ocean system. J Quant Spectrosc Radiat Transfer 2010;111:878–94.
[17] Zhai P-W, Hu Y, Chowdhary J, Trepte CR, Lucker PL, Josset DB. A vector radiative transfer model for coupled atmosphere and ocean systems with a rough interface. J Quant Spectrosc Radiat Transf 2010;111:1025–40.
[18] Garcia RDM, Siewert CE. A simplified implementation of the discrete-ordinates method for a class of problems in radiative transfer with polarization. J Quant Spectrosc Radiat Transf 2011;112:2801–13.
[19] Rozanov VV, Rozanov AV, Kokhanovsky AA, Burrows JP. Radiative transfer through terrestrial atmosphere and ocean: software package SCIATRAN. J Quant Spectrosc Radiat Transf 2014;133:13–71.
[20] Mishchenko MI, Dlugach JM, Chowdhary J, Zaharova NT. Polarized bidirectional reflectance of optically thick sparse particulate layers: an efficient numerically exact radiative-transfer solution. J Quant Spectrosc Radiat Transfer 2015;156:97–108.
[21] Kuščer I, Ribarič M. Matrix formalism in the theory of diffusion of light. Opt Acta 1959;6:42–51.
[22] Domke H. The expansion of scattering matrices for an isotropic medium in generalized spherical functions. Astrophys Space Sci 1974;29:379–86.
[23] Siewert CE. On the equation of transfer relevant to the scattering of polarized light. Astrophys J 1981;245:1080–6.
[24] Siewert CE. On the phase matrix basic to the scattering of polarized light. Astron Astrophys 1982;109:195–200.
[25] Hovenier JW, van der Mee CVM. Fundamental relationships relevant to the transfer of polarized light in a scattering atmosphere. Astron Astrophys 1983;128:1–16.
[26] Hovenier JW, van der Mee C, Domke H. Transfer of polarized light in planetary atmospheres–basic concepts and practical methods. Dordrecht, The Netherlands: Kluwer; 2004.
[27] Domke H. Fourier expansion of the phase matrix for Mie scattering. Z Meteorol 1975;25:357–61.
[28] de Rooij WA, van der Stap CCAH. Expansion of Mie scattering matrices in generalized spherical functions. Astron Astrophys 1984;131:237–48.
[29] Mishchenko MI. Expansion of scattering matrix in generalized spherical functions for radially inhomogeneous spherical particles. Kinem Phys Celest Bodies 1990;6(1):93–5.
[30] Mishchenko MI, Travis LD, Lacis AA. Scattering, absorption, and emission of light by small particles. Cambridge, UK: Cambridge University Press; 2002.
[31] Sanghavi S. Revisiting the Fourier expansion of Mie scattering matrices in generalized spherical functions. J Quant Spectrosc Radiat Transf 2014;136:16–27.
[32] Mishchenko MI, Travis LD. Capabilities and limitations of a current FORTRAN implementation of the T-matrix method for randomly oriented rotationally symmetric scatterers. J Quant Spectrosc Radiat Transf 1998;60:309–24.
[33] Mishchenko MI, Mackowski DW. Light scattering by randomly oriented bispheres. Opt Lett 1994;19:1604–6.
[34] Mackowski DW, Mishchenko MI. Calculation of the T matrix and the scattering matrix for ensembles of spheres. J Opt Soc Am A 1996;13:2266–78.
[35] Mackowski DW, Mishchenko MI. A multiple sphere T-matrix Fortran code for use on parallel computer clusters. J Quant Spectrosc Radiat Transf 2011;112:2182–92.
[36] Mackowski DW. A general superposition solution for electromagnetic scattering by multiple spherical domains of optically active media. J Quant Spectrosc Radiat Transf 2014;133:264–70.
[37] Mishchenko MI, Travis LD, Mackowski DW. *T*-Matrix codes for computing electromagnetic scattering by nonspherical and aggregated particles. ⟨http://www.giss.nasa.gov/staff/mmishchenko/t_matrix.html⟩.
[38] Kahnert M. The T-matrix code *Tsym* for homogeneous dielectric particles with finite symmetries. J Quant Spectrosc Radiat Transf 2013;123:62–78.
[39] Kahnert M. T matrix code for scattering by homogeneous particles with discrete symmetries. ⟨http://www.rss.chalmers.se/~kahnert/Tsym.html⟩.

[40] Quirantes A. Light scattering properties of spheroidal coated particles in random orientation. J Quant Spectrosc Radiat Transf 1999;63:263–75.
[41] Bi L, Yang P, Kattawar GW, Mishchenko MI. Efficient implementation of the invariant imbedding T-matrix method and the separation of variables method applied to large nonspherical inhomogeneous particles. J Quant Spectrosc Radiat Transf 2013;116:169–83.
[42] Bi L, Yang P, Kattawar GW, Mishchenko MI. A numerical combination of extended boundary condition method and invariant imbedding method applied to light scattering by large spheroids and cylinders. J Quant Spectrosc Radiat Transf 2013;123:17–22.
[43] Bi L, Yang P. Accurate simulation of the optical properties of atmospheric ice crystals with the invariant imbedding T-matrix method. J Quant Spectrosc Radiat Transf 2014;138:17–35.
[44] Gustafson BÅS. Microwave analog to light scattering measurements: a modern implementation of a proven method to achieve precise control. J Quant Spectrosc Radiat Transf 1996;55:663–72.
[45] Hovenier JW. Measuring scattering matrices of small particles at optical wavelengths. In: Mishchenko MI, Hovenier JW, Travis LD, editors. Light scattering by nonspherical particles: theory, measurements, and applications. San Diego: Academic Press; 2000. p. 355–65.
[46] Gustafson BÅS. Microwave analog to light-scattering measurements. In: Mishchenko MI, Hovenier JW, Travis LD, editors. Light scattering by nonspherical particles: theory, measurements, and applications. San Diego: Academic Press; 2000. p. 367–90.
[47] Volten H, Muñoz O, Hovenier JW, Waters LBFM. An update of the Amsterdam Light Scattering Database. J Quant Spectrosc Radiat Transf 2006;100:437–43.
[48] Muñoz O, Volten H. Experimental light scattering matrices from the Amsterdam Light Scattering Database. Light Scatter Rev 2006;1:3–29.
[49] Macke A, Mueller J, Raschke E. Scattering properties of atmospheric ice crystals. J Atmos Sci 1996;53:2813–25.
[50] Macke A, Mishchenko MI. Applicability of regular particle shapes in light scattering calculations for atmospheric ice particles. Appl Opt 1996;35:4291–6.
[51] Yang P, Liou KN. Geometric-optics–integral-equation method for light scattering by nonspherical ice crystals. Appl Opt 1996;35:6568–84.
[52] Muinonen K, Nousiainen T, Fast P, Lumme K, Peltoniemi JI. Light scattering by Gaussian random particles: ray optics approximation. J Quant Spectrosc Radiat Transf 1996;55:577–601.
[53] Liou KN, Takano Y, Yang P. Light scattering and radiative transfer in ice crystal clouds: applications to climate research. In: Mishchenko MI, Hovenier JW, Travis LD, editors. Light scattering by nonspherical particles: theory, measurements, and applications. San Diego: Academic Press; 2000. p. 417–49.
[54] Macke A. Monte Carlo calculations of light scattering by large particles with multiple internal inclusions. In: Mishchenko MI, Hovenier JW, Travis LD, editors. Light scattering by nonspherical particles: theory, measurements, and applications. San Diego: Academic Press; 2000. p. 309–22.
[55] Yang P, Liou KN. Light scattering and absorption by nonspherical ice crystals. Light Scatter Rev 2006;1:31–71.
[56] Bi L, Yang P. Physical-geometric optics hybrid methods for computing the scattering and absorption properties of ice crystals and dust aerosols. Light Scatter Rev 2013;8:69–114.
[57] Borovoi A, Konoshonkin A, Kustova N. The physical-optics approximation and its application to light backscattering by hexagonal ice crystals. J Quant Spectrosc Radiat Transf 2014;146:181–9.
[58] Draine BT, Flatau PJ. Discrete dipole approximation for scattering calculations. J Opt Soc Am A 1994;11:1491–9.
[59] Draine BT. The discrete dipole approximation for light scattering by irregular targets. In: Mishchenko MI, Hovenier JW, Travis LD, editors. Light scattering by nonspherical particles: theory, measurements, and applications. San Diego: Academic Press; 2000. p. 131–45.
[60] Yurkin MA, Hoekstra AG. The discrete dipole approximation: an overview and recent developments. J Quant Spectrosc Radiat Transf 2007;106:558–89.
[61] Yurkin MA, Hoekstra AG. The discrete-dipole-approximation code ADDA: capabilities and known limitations. J Quant Spectrosc Radiat Transf 2011;112:2234–47.
[62] Yang P, Liou KN. Finite difference time domain method for light scattering by nonspherical and inhomogeneous particles. In: Mishchenko MI, Hovenier JW, Travis LD, editors. Light scattering by nonspherical particles: theory, measurements, and applications. San Diego: Academic Press; 2000. p. 173–221.
[63] Taflove A, Hagness SC. Computational electrodynamics: the finite-difference time-domain method. Boston: Artech House; 2005.
[64] Inan US, Marshall RA. Numerical electromagnetics: the FDTD method. Cambridge, UK: Cambridge University Press; 2011.
[65] Panetta RL, Liu C, Yang P. A pseudo-spectral time domain method for light scattering computation. Light Scatter Rev 2013;8:139–88.
[66] Liu C, Panetta RL, Yang P. Inhomogeneity structure and the applicability of effective medium approximations in calculating light scattering by inhomogeneous particles. J Quant Spectrosc Radiat Transf 2014;146:331–48.
[67] Volakis JL, Chatterjee A, Kempel LC. Finite element method for electromagnetics. New York: IEEE Press; 1998.
[68] Wriedt T, editor. Generalized multipole techniques for electromagnetic and light scattering. Amsterdam: Elsevier; 1999.
[69] Jin J. The finite element method in electromagnetics. New York: Wiley; 2002.
[70] Kahnert FM. Numerical methods in electromagnetic scattering theory. J Quant Spectrosc Radiat Transf 2003;79–80:775–824.
[71] Doicu A, Wriedt T, Eremin YuA. Light scattering by systems of particles. Null-field method with discrete sources: theory and programs. Berlin: Springer; 2006.
[72] Farafonov VG, Il'in VB. Single light scattering: computational methods. Light Scatter Rev 2006;1:125–77.
[73] Quinten M. Optical properties of nanoparticle systems. Weinheim, Germany: Wiley-VCH; 2011.
[74] Rother T, Kahnert M. Electromagnetic wave scattering on nonspherical particles. Basic methodology and simulations. Berlin: Springer; 2014.
[75] Varshalovich DA, Moskalev AN, Khersonskii VK. Quantum theory of angular momentum. Singapore: World Scientific; 1988.
[76] Krylov VI. Approximate calculation of integrals. New York: Macmillan; 1962.
[77] Mishchenko MI, Zakharova NT. FORTRAN codes for the computation of (polarized) bidirectional reflectance of flat particulate layers and rough surfaces. ⟨http://www.giss.nasa.gov/staff/mmishchenko/brf⟩.
[78] Baum BA, Yang P, Heymsfield AJ, Platnick S, King MD, Hu YX, Bedka ST. Bulk scattering properties for the remote sensing of ice clouds. 2: Narrowband models. J Appl Meteorol 2005;44:1896–911.
[79] Mishchenko MI, Rossow WB, Macke A, Lacis AA. Sensitivity of cirrus cloud albedo, bidirectional reflectance and optical thickness retrieval accuracy to ice particle shape. J Geophys Res 1996;101:16973–85.
[80] Platnick S, Meyer KG, King MD, Wind G, Amarasinghe N, Marchant B, et al. The MODIS cloud optical and microphysical products: updates for Collection 6 and examples from Terra and Aqua. IEEE Trans Geosci Remote Sens 2016 [submitted for publication].